



Published in final edited form as:

Biotechniques. ; 57(5): 241–244. doi:10.2144/000114226.

Nuclear LC3-positive puncta in stressed cells do not represent autophagosomes

Erin M. Buckingham, John E. Carpenter, Wallen Jackson, and Charles Grose

Virology Laboratory, University of Iowa Children's Hospital, Iowa City, IA

Keywords

varicella-zoster virus; herpes virus; autophagy; lysosome; autophagosome; confocal microscopy; Triton X-100

This letter points out an important potential artifact when using immunolabeling techniques with confocal microscopy to identify autophagosomes. Our laboratory has been investigating autophagy induced by varicella-zoster virus (VZV), a human herpesvirus. Although closely related to herpes simplex virus type 1 (HSV-1), VZV lacks the inhibitors of autophagy harbored within the HSV genome (1), (2), (3). Therefore, autophagy is abundant after VZV infection (4), (5), (6). Many of our studies have relied upon autophagosome quantitation to gauge the level of autophagy under varying conditions of infection (7). For these assays, we have enumerated autophagosomes (puncta) in the cytoplasm after immunolabeling with commercial LC3 antibody reagents (7). Depending on the conditions, we occasionally noticed what appeared to be puncta in the nuclei of the infected cells. In two recent autophagy articles (8), (9), other investigators had identified LC3-positive puncta in the nuclei of their stressed cells. They have implied that these LC3-positive puncta may be related to autophagy. Based on our extensive observations investigating VZV-induced autophagy, we postulate that these nuclear puncta are not related to autophagosome production, but instead are related to the antibody reagent and other experimental conditions under which the microscopy experiment is carried out.

Based on prior autophagy experiments in our laboratory, we first postulated that different anti-LC3 antibodies led to different levels of nuclear LC3 staining. The panels of Figure 1 illustrate the main differences between using a rabbit monoclonal antibody (Epitomics #2057-1) versus a rabbit polyclonal antibody (Santa Cruz #sc-28266) in different cell lines. In immortalized human keratinocytes (TERT-HFK), both uninfected and VZV-infected cells were labeled with anti-LC3 antibodies, but there was a much greater amount of nuclear LC3 staining with the rabbit polyclonal anti-LC3 reagent (compare panels A and B). Panel D

Corresponding author: Charles Grose (charles-grose@uiowa.edu), University Hospital/2501JCP, 200 Hawkins Drive, Iowa City, IA 52242, TEL: 319-356-2270/356-4855.

AUTHOR CONTRIBUTIONS

E.M.B. designed experiments, obtained and analyzed data, and prepared manuscript. J.E.C. and W.J. contributed to study design, obtained and analyzed data, and contributed to manuscript preparation. C.G. supervised study and prepared manuscript.

COMPETING INTERESTS STATEMENT: The authors declare no competing interests.

demonstrates that VZV IE62 immunoreactivity (red), an abundant viral protein, was present in panel B.

Panels E and F of Figure 1 show similar results in melanoma cells (4). Panel E shows syncytia cytopathology induced by VZV infection. Interestingly, nuclei (blue color) within the syncytia did not show LC3 staining after immunolabeling with the rabbit monoclonal antibody (E), although cytoplasmic puncta were easily seen. In contrast, immunolabeling with the rabbit polyclonal antibody caused prominent nuclear LC3 staining, as noted by the green puncta within the blue nuclei (F). Similar nuclear LC3 patterns were also seen in infected MRC-5 fibroblasts after immunolabeling with a polyclonal reagent (not shown). In short, nuclear puncta were more easily seen with polyclonal anti-LC3 reagents, regardless of the infected cell substrate.

We next postulated that the conditions for permeabilization of the cells before immunolabeling were very important to the level of nuclear LC3 staining. All articles cited above have used Triton X-100 for permeabilization. In previous experiments, we have used Triton concentrations ranging from 0.02% to 0.1% for one hour at room temperature (RT), to permeabilize cells before immunolabeling with LC3 antibody. In the experiment shown in Figure 1 (G–I), infected cells were fixed with 2% paraformaldehyde and permeabilized with 0.02% (G), 0.05% (H) or 0.1% (I) Triton X-100, then immunolabeled with the rabbit polyclonal antibody against LC3. As the amount of Triton X-100 was increased, more nuclei contained LC3 staining. Note in particular that almost every blue nucleus in panel I contained green puncta. This effect had been observed in many different experiments in this laboratory, using different cell types and conditions of infection. We also observed that some nuclear puncta were larger than typically seen in the cytoplasm of VZV-infected cells, namely, true cytoplasmic puncta are $590 \text{ nm} \pm 240 \text{ nm}$ (10) whereas some nuclear puncta were $>1000 \text{ nm}$ in diameter.

After observing the above differences between cytoplasmic and nuclear puncta, we postulated that the nuclear puncta were not typical double-membraned autophagosomes. Since our laboratory has used transmission electron microscopy (TEM) to examine virus-infected cells for many years, we have a large archive of micrographs. We have already documented cytoplasmic autophagosomes by TEM in an earlier paper (5). For this report, we re-examined over 70 micrographs to look for any structures that resembled autophagosomes within the nuclei of uninfected or infected cells (Figure 2). In virus-infected monolayers during later timepoints (11), many viral capsids were seen in the nuclei; capsids measure 75–100 nm in diameter (5). Since autophagosomes typically are 4–6 fold larger, we should be able to easily identify these structures, if they were present in the nuclei of these cells (Figure 2, E–H). Note the diameter of a virion in a cytoplasmic vacuole as another size control (Figure 2, circled in H). However, we found no double-membraned structures within nuclei (Figure 2). We also examined nuclear preparations from uninfected MRC-5 fibroblasts for the presence of structures that resembled autophagosomes. As seen in representative TEM images in Figure 2 (A–D), no double-membraned structures were found in uninfected nuclei. Therefore, punctate LC3 staining within nuclei of cells was not due to the LC3-II embedded in the membrane of autophagosomes or an organelle resembling an autophagosome.

We were intrigued when we read two recent autophagy papers in which the authors had observed what were called nuclear puncta identified by various anti-LC3 antibody reagents (8), (9). The authors were uncertain as to their function but speculated that the nuclear puncta may be related to autophagy. We know of no reason why our data about VZV-induced autophagy should not be applicable broadly. In particular, viral capsids in the nucleus provide a valuable marker for any structures >100 nm. Yet we see no structures compatible in size with autophagosomes in nuclei. Based on data acquired in our VZV-induced autophagy system, therefore, we postulate that these nuclear puncta are not related to autophagosome production.

Instead, we conclude that a likely explanation for nuclear puncta is the formation of LC3 aggregates within the nuclei and their detection by the primary anti-LC3 antibody reagent (12). LC3-II protein is easily detectable in the nucleus (13). Earlier studies of direct precipitation of antigen by antibody by this laboratory and others demonstrate that aggregates are readily bound by polyclonal antisera (14). Further, aggregate detection is more pronounced with polyclonal as opposed to monoclonal antibody reagents. In addition, the nonionic detergent Triton X-100 does not hinder the detection of antigen-antibody aggregates at the concentrations used for permeabilization (15).

Finally, we note that we are not advising that polyclonal anti-LC3 antibody reagents be avoided in autophagy studies. We are pointing out the optimal experimental conditions for their use in the detection of cytoplasmic puncta by confocal microscopy techniques.

Acknowledgments

We thank A. Klingelutz (University of Iowa) for his gift of the TERT-HFK cells. This autophagy research was supported by NIH grant AI89716 (C.G.). The University of Iowa Central Microscopy Research Facility is supported by NIH grant 1S10RR025439. This paper is subject to the NIH Public Access Policy.

References

1. Gobeil PA, Leib DA. Herpes simplex virus gamma 34.5 interferes with autophagosome maturation and antigen presentation in dendritic cells. *MBio*. 2012; 3
2. Davison AJ, Scott JE. The complete DNA sequence of varicella-zoster virus. *J Gen Virol*. 1986; 67:1759–1816. [PubMed: 3018124]
3. Orvedahl A, Alexander D, Tallozy Z, Sun Q, Wei Y, Zhang W, Burns D, Leib DA, Levine B. HSV-1 ICP34.5 confers neurovirulence by targeting the Beclin 1 autophagy protein. *Cell Host Microbe*. 2007; 1:23–35. [PubMed: 18005679]
4. Carpenter JE, Jackson W, Benetti L, Grose C. Autophagosome formation during varicella-zoster virus infection following endoplasmic reticulum stress and the unfolded protein response. *J Virol*. 2011; 85:9414–9424. [PubMed: 21752906]
5. Takahashi MN, Jackson W, Laird DT, Culp TD, Grose C, Haynes JI 2nd, Benetti L. Varicella-zoster virus infection induces autophagy in both cultured cells and human skin vesicles. *J Virol*. 2009; 83:5466–5476. [PubMed: 19297471]
6. Buckingham EM, Carpenter JE, Jackson W, Grose C. Autophagy and the effects of its inhibition on varicella-zoster virus glycoprotein biosynthesis and infectivity. *J Virol*. 2014; 88:890–902. [PubMed: 24198400]
7. Klionsky DJ, Abdalla FC, Abeliovich H, Abraham RT, Acevedo-Arozena A, Adeli K, Agholme L, Agnello M, et al. Guidelines for the use and interpretation of assays for monitoring autophagy. *Autophagy*. 2012; 8:445–544. [PubMed: 22966490]

8. Martinez-Lopez N, Athonvarangkul D, Mishall P, Sahu S, Singh R. Autophagy proteins regulate ERK phosphorylation. *Nat Commun.* 2013; 4:2799. [PubMed: 24240988]
9. Corum DG, Tschlis PN, Muise-Helmericks RC. AKT3 controls mitochondrial biogenesis and autophagy via regulation of the major nuclear export protein CRM-1. *FASEB J.* 2014; 28:395–407. [PubMed: 24081905]
10. Jackson W, Yamada M, Moninger T, Grose C. Visualization and quantitation of abundant macroautophagy in virus-infected cells by confocal three-dimensional fluorescence imaging. *J Virol Methods.* 2013; 193:244–250. [PubMed: 23792686]
11. Hutchinson, JA. Interdisciplinary Studies. University of Iowa; Iowa City, IA: 2007. Thesis: Imaging analysis of varicella-zoster virus infection with emphasis on glycoprotein C; p. 224
12. Kuma A, Matsui M, Mizushima N. LC3, an autophagosome marker, can be incorporated into protein aggregates independent of autophagy: caution in the interpretation of LC3 localization. *Autophagy.* 2007; 3:323–328. [PubMed: 17387262]
13. Karim MR, Kanazawa T, Daigaku Y, Fujimura S, Miotto G, Kadowaki M. Cytosolic LC3 ratio as a sensitive index of macroautophagy in isolated rat hepatocytes and H4-II-E cells. *Autophagy.* 2007; 3:553–560. [PubMed: 17617739]
14. Horwitz, MS.; Scharff, MD. Immunological precipitation of radioactively labeled viral proteins. In: Habel, K.; Salzman, NP., editors. *Fundamental Techniques in Virology.* Academic Press; New York, NY: 1969. p. 297-315.
15. Qualtiere LF, Anderson AG, Meyers P. Effects of ionic and nonionic detergents on antigen-antibody reactions. *J Immunol.* 1977; 119:1645–1651. [PubMed: 410880]

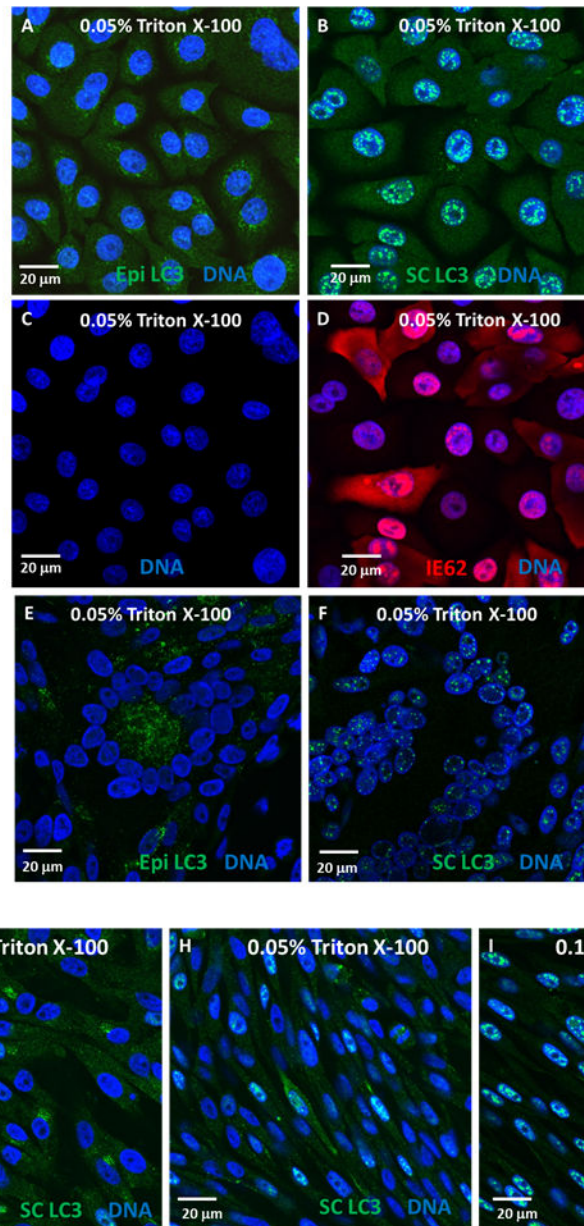


Figure 1.

Effects of antibody choice and permeabilization on nuclear LC3 immunoreactivity. (A–D) TERT-HFK cells, uninfected (A&C) or virus-infected (B&D), were permeabilized with 0.05% Triton X-100 and labeled with either Epitomics rabbit monoclonal anti-LC3 (Epi LC3; A) or Santa Cruz rabbit polyclonal anti-LC3 (SC LC3; B) (green), MAb 5C6 against VZV IE62 protein (red) (D), and the blue fluorescent H33342 DNA stain (Invitrogen) (A–D). Infections and immunolabeling were performed as described (6). Briefly, cells were grown on glass coverslips in 6-well dishes. After infection, monolayers were fixed, permeabilized and blocked in 5% nonfat milk with 2.5% normal goat serum in PBS for 2 h. Cells were then immunolabeled (primary antibody overnight at 4°C; secondary antibody for 2 h at RT). Coverslips were mounted on glass slides and viewed on a Zeiss 710 Laser

Scanning Confocal Microscope. Images were analyzed using Zen 2009 (Zeiss) software. LC3 puncta were seen in the cytoplasm of TERT-HFK cells when labeled with a rabbit monoclonal antibody against LC3 (A), but a rabbit polyclonal antibody against LC3 labeled mostly puncta in the nucleus, with some cytoplasmic staining (B). (E&F) Infected melanoma cells were permeabilized with 0.05% Triton X-100, and labeled with DNA stain (blue) and either Epitomics rabbit monoclonal anti-LC3 (Epi LC3; E) or Santa Cruz rabbit polyclonal anti-LC3 (SC LC3; F). In these cells, the monoclonal antibody labeled mainly cytoplasmic LC3 (E), while the polyclonal antibody stained primarily nuclear LC3 (F). (G–I) Three infected melanoma monolayers were fixed and permeabilized with increasing amounts of Triton X-100: 0.02% (G), 0.05% (H), or 0.1% (I), then labeled with a rabbit polyclonal antibody to LC3 (green) and the DNA stain (blue). While occasional nuclei showed some LC3 staining at 0.02% Triton X-100 concentration, nuclear LC3 staining increased greatly from 0.05% to 0.1%. All images are shown are at a final magnification of 630X, and all scale bars represent 20 μm .

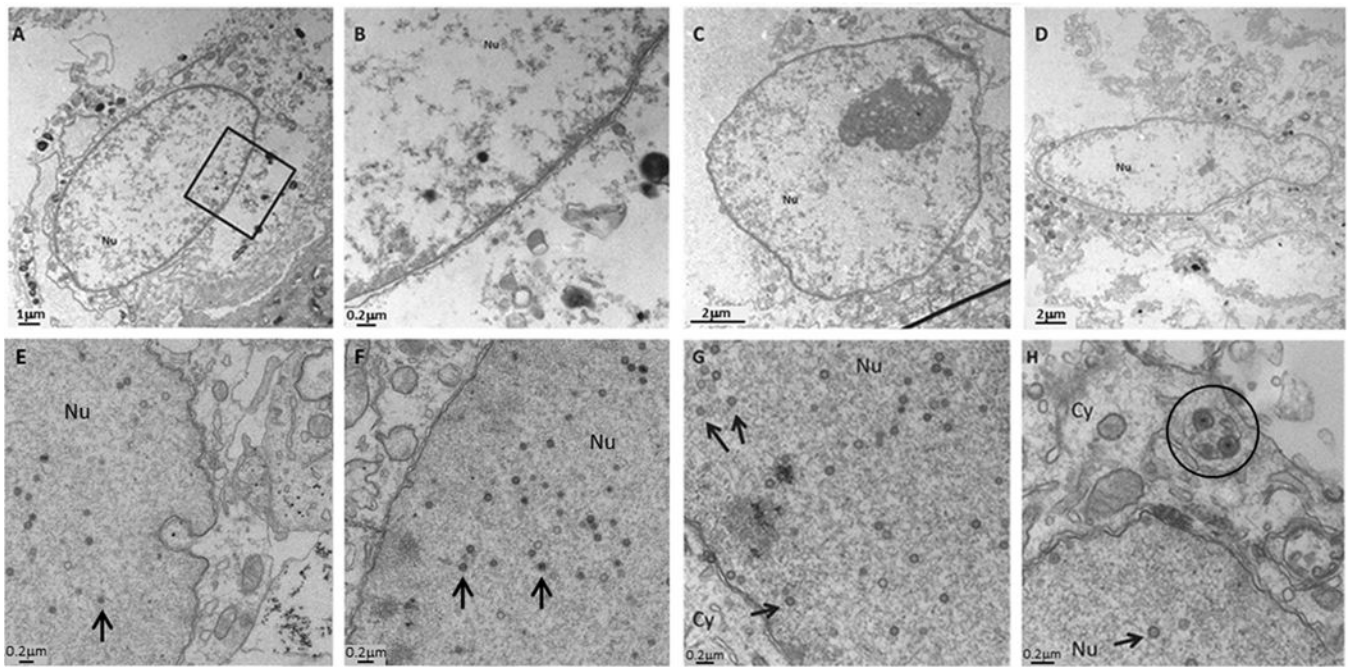


Figure 2.

Absence of double-membraned autophagosomal structures in electron micrographs of nuclei of uninfected and virus-infected cells. (A–D) Nuclei isolated from uninfected cells showed no double-membraned structures resembling autophagosomes when examined by TEM. Panel B is a magnification of the region within the black box in panel A. (E–H) Melanoma cells infected with VZV showed no autophagosomal-like structures in the nucleus. Cells were infected for 24 h (E) or 72 h (F–H) and imaged by TEM. Black arrows within nuclei point to viral capsids of approximately 75–100 nm diameter. Circle in panel (H) encloses virions within a cytoplasmic vacuole. Nu = nucleus; Cy = cytoplasm. Scale bars included in each panel.